NUMERICAL LINEAR ALGEBRA WITH APPLICATIONS
Numer. Linear Algebra Appl. 2008; **15**:661–683
Published online 17 March 2008 in Wiley InterScience (www.interscience.wiley.com). DOI: 10.1002/nla.587

Distributive smoothers in multigrid for problems with dominating grad–div operators

F. J. Gaspar[1,*,†], J. L. Gracia[1], F. J. Lisbona[1] and C. W. Oosterlee[2,3]

[1]*Applied Mathematics Department, University of Zaragoza, Zaragoza, Spain*
[2]*CWI—Center for Mathematics and Computer Science, Amsterdam, The Netherlands*
[3]*Delft Institute of Applied Mathematics (DIAM), Delft University of Technology, Delft, The Netherlands*

SUMMARY

In this paper, we present efficient multigrid methods for systems of partial differential equations that are governed by a dominating grad–div operator. In particular, we show that distributive smoothing methods give multigrid convergence factors that are independent of problem parameters and of the mesh sizes in space and time. The applications range from model problems to secondary consolidation Biot's model. We focus on the smoothing issue and mainly solve academic problems on Cartesian-staggered grids. Copyright © 2008 John Wiley & Sons, Ltd.

Received 5 September 2007; Revised 31 December 2007; Accepted 23 January 2008

KEY WORDS: multigrid; distributive smoothing; grad–div operator; staggered grid; poro-elasticity

1. INTRODUCTION

In this paper, we consider distributive smoothing methods for the multigrid solution of systems of partial differential equations (PDEs) and deal, in particular, with operators that contain a dominating gradient–divergence (grad–div) term. The gradient–divergence operator appears frequently in the formulation of mathematical models in physics and engineering, such as in fluid flow, solid mechanics, magnetohydrodynamics, or electromagnetism problems. Sometimes, this operator is used to improve the numerical properties of particular discrete models. For example, Olshanskii

*Correspondence to: F. J. Gaspar, Applied Mathematics Department, Centro Politecnico Superior, C/Maria de Luna 3, 50018-Zaragoza, Spain.
†E-mail: fjgaspar@unizar.es

Contract/grant sponsor: ICT Project BRICKS
Contract/grant sponsor: Spanish project MTM 2004-019051; contract/grant number: 019051

and Reusken [1] showed that the grad–div term has a stabilization effect on the discrete Stokes equations. This process was called 'grad–div stabilization'.

Our interest lies in the efficient solution of some boundary-value problems governed by a dominating grad–div operator by the multigrid solution method. Unfortunately, the usual multigrid smoothers are not effective when applied to the grad–div problems considered here. As it was pointed out, for example, in [2], the eigenspace associated with the minimal eigenvalue of the discrete operator contains many eigenvectors, as any divergence-free vector is an eigenvector corresponding to this minimal eigenvalue. These can be arbitrary oscillatory and can neither be reduced by standard smoothing procedures nor be well represented on coarse grids.

Vassilevski and Wang [3] studied multigrid methods for solving the discrete system of equations with a dominating grad–div term. Their approach builds upon local div–free functions and their orthogonal complements in the finite element space. Arnold *et al.* [4] presented a multigrid preconditioner for a discrete system of equations which arises when discretizing the variational formulation of a grad–div equation with the lowest-order Raviart–Thomas finite element spaces on triangles. We also point to the work by Hiptmair and Hoppe [5], who present a technique that is essentially distributive smoothing in a finite element context to handle the troublesome div-free components. Although in finite elements special elements have been proposed for this purpose, in finite differences a stable discretization can be achieved by means of grid staggering.

In a series of papers, with different co-authors, we aim at solving systems of PDEs in a robust and efficient way with the multigrid solution method. The systems of interest were often discrete versions of the poroelasticity system, either discretized on a staggered or on a vertex-centered grid. In the latter case, we developed stabilization techniques, for example, by first reformulating the continuous system, so that the transformed system leads to a stable scheme in a natural way.

One focus of the poroelasticity system has been on a robust and efficient multigrid distributive smoothing method that resulted in a decoupled treatment of the different equations of the PDE system during smoothing. As distributive smoothing methods are based on manipulations with discrete operators, they have, in our experience so far, mainly been successful for *mimetic* discretizations [6, 7]. An example is the staggered grid discretization, which mimics the properties and action of continuous divergence and gradient operators under operator transformations.

In this paper, we continue our search for efficient distributive smoothers, this time for problems with dominating gradient–divergence operators. We focus on a staggered grid arrangement for discretization, for which the convergence of discrete schemes has been proved rigorously [8, 9]. We mention that the well-known local Fourier analysis (LFA) [10, 11] can also successfully be applied to develop efficient multigrid methods for systems of PDEs with constant (or frozen) coefficients. We do not use it in this paper; see, however, [12] for LFA results in the case of distributive smoothing for systems of PDEs.

The plan of the paper is as follows. In Section 2, we discuss the multigrid methods and the concept of distributive smoothing, in particular, with the help of a simple model system of equations. In the sections to follow, a variety of systems of equations, each with a dominating grad–div operator, are discussed, and the corresponding distributive smoothing methods are introduced. Each section contains some numerical experiments on model problems. In Section 3, we discuss linear elasticity for nearly incompressible materials, discretized on a staggered grid. Sections 4 and 5 focus on consolidation problems with poroelasticity models. There we discuss both linear poroelasticity and secondary consolidation models and define the proper distributive smoothers. Most of the problems are academic test problems with analytic solutions, but the last section also discusses a 3D linear poroelasticity experiment with realistic stress boundary conditions.

DOI: 10.1002/nla

2. DISTRIBUTIVE SMOOTHING IN MULTIGRID FOR A MODEL PROBLEM

In this section, we describe and motivate our choice of multigrid smoother with the help of a simple model system of equations containing a large parameter λ:

$$-\lambda \mathbf{grad}\,\mathrm{div}\,\mathbf{u}+\mathbf{u}=\mathbf{f} \quad \text{in } \Omega \tag{1}$$

where Ω is an open domain in R^2, λ is positive, and $\mathbf{f}\in L^2(\Omega)^2$. The essential boundary condition is given by $\mathbf{u}\cdot\mathbf{n}=0$ on $\partial\Omega$, where $\mathbf{n}$ denotes the outer unit normal vector along the boundary $\partial\Omega$. Another relevant boundary condition is $\mathrm{div}\,\mathbf{u}=0$, which is the natural boundary condition. With these boundary conditions, the corresponding boundary-value problem obviously has a unique solution in $H(\mathrm{div})$. One application of problem (1) is during the implementation of the sequential regularization method (SRM) for the unsteady incompressible Navier–Stokes system, introduced in [13]. The SRM method requires the solution of an equation of the form (1) at each time step. In the framework of finite element methods, Arnold *et al.* [2] proved the convergence of efficient multigrid methods using appropriate finite element spaces (Raviart–Thomas–Nedelec) and appropriate smoothers. In the finite difference context, we will use mimetic discretizations on staggered grids and distributive smoothers in order to obtain robust multigrid methods.

2.1. Discretization

We start defining the different grids and discrete operators used in the discretization of (1). As the spatial domain, we consider the unit square $\Omega=(0,1)^2$ and for simplicity all the grids will be uniform with the same mesh size h in both directions. We introduce the following meshes:

$$\begin{aligned}
\overline{\omega}_n &= \{(ih, jh),\ i,j=0,\ldots,N\}\\
\overline{\omega}_u &= \{((i+\tfrac{1}{2})h, jh),\ i=-\tfrac{1}{2},0,1,\ldots,N-1,N-\tfrac{1}{2},\ j=0,\ldots,N\}\\
\overline{\omega}_v &= \{(ih, (j+\tfrac{1}{2})h),\ i=0,\ldots,N,\ j=-\tfrac{1}{2},0,1,\ldots,N-1,N-\tfrac{1}{2}\}\\
\omega_c &= \{((i+\tfrac{1}{2})h, (j+\tfrac{1}{2})h),\ i,j=0,1,\ldots,N-1\}
\end{aligned} \tag{2}$$

where $h=1/N$ and N is a positive integer (see Figure 1).

Let us denote by ω_n, ω_u, and ω_v the set of interior nodes and by $\partial\omega_n, \partial\omega_u$, and $\partial\omega_v$ the set of boundary nodes of $\overline{\omega}_n, \overline{\omega}_u$, and $\overline{\omega}_v$, respectively. $H_{\overline{\omega}_n}, H_{\overline{\omega}_u}, H_{\overline{\omega}_v}$, and H_{ω_c} then denote the spaces

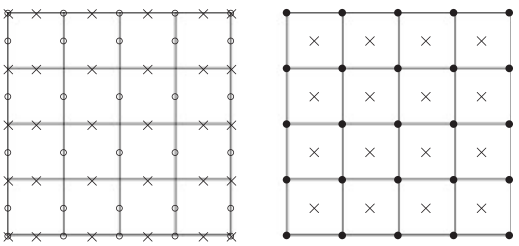

Figure 1. Grids $\overline{\omega}_u\times$ and $\overline{\omega}_v\circ$ (left picture) and grids $\overline{\omega}_n\bullet$ and $\omega_c\times$ (right picture).

DOI: 10.1002/nla

of grid functions defined on $\overline{\omega}_n, \overline{\omega}_u, \overline{\omega}_v$, and ω_c, respectively, and $H_{\omega_n}, H_{\omega_u}$, and H_{ω_v} are the subspaces of $H_{\overline{\omega}_n}, H_{\overline{\omega}_u}$, and $H_{\overline{\omega}_v}$ of grid functions vanishing at the boundaries.

Next, we define discrete operators and start with the discrete divergence operator, $\mathrm{div}_h : H_{\overline{\omega}_u} \times H_{\overline{\omega}_v} \to H_{\overline{\omega}_n}$, which is defined in 2D by

$$(\mathrm{div}_h \mathbf{u})_{i,j} = (u_x)_{i,j} + (v_y)_{i,j}, \quad i, j = 0, \ldots, N$$

where for the interior points,

$$(u_x)_{i,j} = h^{-1}(u_{i+1/2,j} - u_{i-1/2,j}), \quad (v_y)_{i,j} = h^{-1}(v_{i,j+1/2} - v_{i,j-1/2})$$

and for the boundary points,

$$(u_x)_{0,j} = 2h^{-1}(u_{1/2,j} - u_{0,j}), \quad j = 0, \ldots, N$$

$$(u_x)_{N,j} = 2h^{-1}(u_{N,j} - u_{N-1/2,j}), \quad j = 0, \ldots, N$$

$$(v_y)_{i,0} = 2h^{-1}(v_{i,1/2} - v_{i,0}), \quad i = 0, \ldots, N$$

$$(v_y)_{i,N} = 2h^{-1}(v_{i,N} - v_{i,N-1/2}), \quad i = 0, \ldots, N$$

The discrete gradient operator $\mathbf{grad}_h : H_{\overline{\omega}_n} \to H_{\overline{\omega}_u} \times H_{\overline{\omega}_v}$ is defined as $\mathbf{grad}_h\, p = (\mathrm{grad}_h^x\, p, \mathrm{grad}_h^y\, p) \in H_{\overline{\omega}_u} \times H_{\overline{\omega}_v}$, where for $j = 0, \ldots, N$,

$$(\mathrm{grad}_h^x\, p)_{i+1/2,j} = \begin{cases} h^{-1}(p_{i+1,j} - p_{i,j}), & i = 0, \ldots, N-1 \\ p_{0,j}, & i = -1/2 \\ -p_{N,j}, & i = N - 1/2 \end{cases}$$

and for $i = 0, \ldots, N$,

$$(\mathrm{grad}_h^y\, p)_{i,j+1/2} = \begin{cases} h^{-1}(p_{i,j+1} - p_{i,j}), & j = 0, \ldots, N-1 \\ p_{i,0}, & j = -1/2 \\ -p_{i,N}, & j = N - 1/2 \end{cases}$$

In the 2D case, we need the following two continuous operators:

$$\mathrm{rot}\,\mathbf{u} = -\frac{\partial u}{\partial y} + \frac{\partial v}{\partial x} \quad \text{and} \quad \mathbf{rot}\,\omega = \left(\frac{\partial w}{\partial y}, -\frac{\partial w}{\partial x}\right)$$

The corresponding discrete operators are defined by, $\mathrm{rot}_h : H_{\overline{\omega}_u} \times H_{\overline{\omega}_v} \to H_{\omega_c}$

$$(\mathrm{rot}_h \mathbf{u})_{i+1/2,j+1/2} = h^{-1}(u_{i+1/2,j} + v_{i+1,j+1/2} - u_{i+1/2,j+1} - v_{i,j+1/2}), \quad i, j = 0, \ldots N-1$$

and

$$\mathbf{rot}_h : H_{\omega_c} \to H_{\omega_u} \times H_{\omega_v}, \quad \mathbf{rot}_h\, w = (\mathrm{rot}_h^x w, \mathrm{rot}_h^y w)$$

$$(\mathrm{rot}_h^x w)_{i+1/2,j} = h^{-1}(w_{i+1/2,j+1/2} - w_{i+1/2,j-1/2})$$

$$(\mathrm{rot}_h^y w)_{i,j+1/2} = h^{-1}(-w_{i+1/2,j+1/2} + w_{i-1/2,j+1/2}), \quad i, j = 1, \ldots, N-1$$

DOI: 10.1002/nla

We note that the grid operators defined previously are consistent with the following continuous properties:

$$\mathrm{rot}\,\mathbf{grad}=0, \quad \mathrm{div}\,\mathbf{rot}=0$$

i.e. $\mathrm{rot}_h\,\mathbf{grad}_h\,p=0,\ \forall p\in H_{\overline{\omega}_n}$, $\mathrm{div}_h\,\mathbf{rot}_h\,w=0, \forall w\in H_{\omega_c}$. With the discrete operators $\mathbf{grad}_h$ and div_h, we easily propose a discrete version of problem (1). Operators rot_h and $\mathbf{rot}_h$ will be useful in the construction of the distributive smoother.

2.2. *Multigrid and smoothing method for model problem*

Here, we develop efficient multigrid solvers for problems discretized on staggered grids. Multigrid methods are widely accepted as highly efficient solvers for PDEs. Owing to the regularly structured grid adopted in this model study, we can choose standard geometric grid coarsening, i.e. the sequence of coarse grids is obtained by doubling the mesh size in each spatial direction, which is indicated by a subscript '$2h$'. The coarse grid correction consists of geometric transfer operators $R_{h,2h}$, $P_{2h,h}$, and a direct coarse grid discretization of the continuous operator. As the prolongation operators $P^u_{2h,h}$ and $P^v_{2h,h}$, we apply the usual interpolation operators based on bilinear interpolation of neighboring staggered grid coarse grid unknowns. At the u- and v-grid points, we consider 6-point restrictions with the nearest neighbors. In stencil notation, they are given by

$$R^u_{h,2h}\mathrel{\hat{=}}\frac{1}{8}\begin{bmatrix}1 & & 1\\ 2 & \star & 2\\ 1 & & 1\end{bmatrix}_h, \quad R^v_{h,2h}\mathrel{\hat{=}}\frac{1}{8}\begin{bmatrix}1 & 2 & 1\\ & \star & \\ 1 & 2 & 1\end{bmatrix}_h$$

respectively, where $\star$ denotes the position on the coarse grid at which the restriction is applied [11]. For the system considered here, there is no benefit in using the Galerkin coarse grid discretization.

Geometric multigrid method yields textbook convergence rates, especially when the reduction of high-frequency components of an error in the numerical approximation is associated with large eigenvalues of an iterative solution method. This is true for matrices generated from common stable discretizations of many nicely elliptic equations and ensures that smoothing methods such as Gauss–Seidel or Jacobi dampen high-frequency error components and thus generate smooth error.

Some of the simplest and most frequently used smoothers for elliptic problems, however, do not yield effective multigrid methods for grad–div problems, because the eigenspace associated with the lowest eigenvalue of the dominating grad–div operators contains many high-frequency eigenfunctions, which cannot be presented well on a coarse mesh.

2.2.1. Distributive smoothing method. Decoupled, i.e. equationwise, smoothing for a discrete system of equations is preferred for reasons of efficiency. If a system of equations consists of elliptic and of other, non-elliptic, equations, decoupled smoothing easily allows us to choose different iterative methods for the different operators appearing in the system. For many systems, however, including those of interest here, equationwise smoothing directly on the original discrete system is not sufficient, as indicated, for example, by LFA smoothing techniques [11]. Instead, one first has to transform the discrete system such that equationwise smoothing on the transformed discrete system, followed by a back-transformation to the original unknowns, brings excellent smoothing factors. Equationwise, decoupled smoothing on a transformed system is called *distributive smoothing*.

DOI: 10.1002/nla

An easy way to describe a distributive smoothing method for $\mathbf{L}_h\mathbf{u}_h=\mathbf{f}_h$, where $\mathbf{L}_h$ represents a discretization of the continuous operator, is by means of a *right preconditioner* [14, 15]. In distributive smoothing methods, we work with a transformed system $\mathbf{L}_h\mathbf{C}_h\mathbf{w}_h=\mathbf{f}_h$ (where $\mathbf{u}_h=\mathbf{C}_h\mathbf{w}_h$), with $\mathbf{C}_h$ chosen such that the operator $\mathbf{L}_h\mathbf{C}_h$ allows a *decoupled* smoothing procedure. Distributive iteration is then given by

$$\mathbf{u}_h^{m+1}=\mathbf{u}_h^m+\mathbf{C}_h\mathbf{B}_h(\mathbf{f}_h-\mathbf{L}_h\mathbf{u}_h^m) \tag{3}$$

with $\mathbf{B}_h\approx(\mathbf{L}_h\mathbf{C}_h)^{-1}$. We choose a basic iterative method, denoted by $\mathbf{B}_h$ above, for smoothing each of the scalar equations of the transformed system.

Distributive smoothing methods for incompressible flow problems have been presented in [14, 16] (see also [11]) and for the poroelasticity system in [17].

Here, we define for the discrete model problem:

$$-\lambda\,\mathbf{grad}_h\,\mathrm{div}_h\,\mathbf{u}_h+\mathbf{u}_h=\mathbf{f}_h \tag{4}$$

with λ large and positive, a distributive smoother that permits us to decouple the unknowns of its associated linear system. We introduce a new variable $\mathbf{w}_h$ such that

$$\mathbf{u}_h=\mathbf{rot}_h\,\mathrm{rot}_h\,\mathbf{w}_h+\frac{1}{\lambda}\mathbf{w}_h \tag{5}$$

Using the consistency properties of the discrete operators, the transformed system reads

$$-\mathbf{grad}_h\,\mathrm{div}_h\,\mathbf{w}_h+\mathbf{rot}_h\,\mathrm{rot}_h\,\mathbf{w}_h+\frac{1}{\lambda}\mathbf{w}_h=\mathbf{f}_h$$

where the first two terms represent the discretization of the vector Laplace operator. If we work in Cartesian coordinates in 2D, the distributor reads

$$\mathbf{C}_h=\begin{pmatrix}-(\partial_{yy})_h+\dfrac{1}{\lambda}I_h & (\partial_{xy})_h\\[2ex] (\partial_{xy})_h & -(\partial_{xx})_h+\dfrac{1}{\lambda}I_h\end{pmatrix}$$

so that we obtain the transformed system:

$$\mathbf{L}_h\mathbf{C}_h=\begin{pmatrix}-\Delta_h+\dfrac{1}{\lambda}I_h & 0\\[2ex] 0 & -\Delta_h+\dfrac{1}{\lambda}I_h\end{pmatrix} \tag{6}$$

where I_h is the discrete identity operator. Note that the transformed system in Cartesian coordinates is diagonal, and the Laplacian-type operators can be smoothed in a decoupled fashion with any efficient smoother for $-\Delta_h$. Think of the well-known scalar version of red–black Gauss–Seidel iteration, for example. In this paper, we will show that the multigrid convergence with distributive smoothing based on transformation (5) converges satisfactorily for large values of λ.

DOI: 10.1002/nla

2.2.2. Coupled smoothing method. Coupled smoothing of unknowns in a staggered grid arrangement is typically done by updating *sets of unknowns* collectively. Pointwise smoothing means in this staggered case 'cellwise' smoothing. A small matrix must be inverted for each cell. A coupled pointwise Gauss–Seidel iteration for the discrete model system would update two unknowns in a staggered arrangement simultaneously. An approach with some success in various applications, however, locally updates all unknowns appearing in the divergence operator simultaneously. For incompressible Navier–Stokes equations, this cellwise smoothing method is called the 'Vanka smoother' after the author of the first paper [18]. For poroelasticity, we evaluated the Vanka smoothers in [17] for staggered grid discretizations and in [19] for stabilized vertex-centered discretizations. For staggered grid discretizations, we found that although distributive smoothing gave excellent multigrid convergence independent of all problem parameters, the coupled smoother showed a convergence dependency on the time step. For very small time steps, the multigrid convergence degraded. An advantage of coupled smoothing was, however, that it also led to satisfactory multigrid convergence on vertex-centered grids, whereas straightforward distributive smoothing did not.

2.2.3. Numerical result for model problem. We end this introduction in multigrid and staggered grids by considering a numerical multigrid experiment for model system (1). We consider distributive smoothing in this section. We will solve discrete equation (4) with $\lambda = 10^4$, on $\Omega = (0, 1)^2$, with right-hand side $f = 1$ and boundary conditions $\mathbf{u} \cdot \mathbf{n} = 0$. The solution is symmetric in the unknowns u and v. Figure 2 presents the u-component of the solution. The solution is large and smooth.

The measure of convergence is related to the absolute value of the residual after the mth iteration in the maximum norm over the two equations in the system:

$$\text{res}_h^m = |r_{1,h}^m| + |r_{2,h}^m|$$

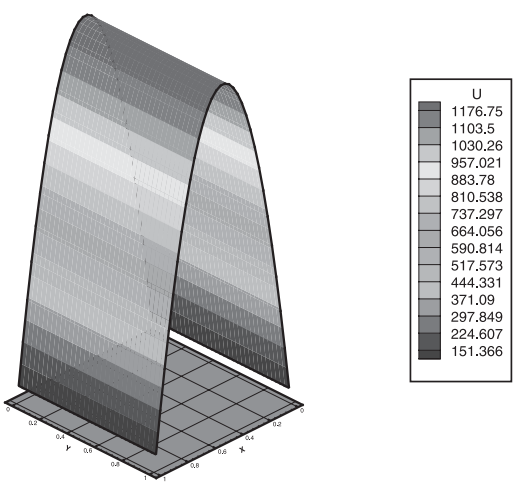

Figure 2. Component u of the numerical solution of the grad–div model problem.

DOI: 10.1002/nla

Table I. $F(1,1)$-multigrid convergence factors, ρ_h, and in brackets, the number of iterations for the model problem (1).

	32×32	64×64	128×128	256×256
$\lambda=1.0$	0.11 (9)	0.11 (9)	0.11 (9)	0.11 (9)
$\lambda=10^2$	0.11 (9)	0.11 (9)	0.11 (9)	0.11 (9)
$\lambda=10^4$	0.11 (9)	0.11 (9)	0.11 (9)	0.11 (9)

where $r^m_{i,h}$ is the residual associated to the ith equation of the system. The average reduction factor ρ_h is given by

$$\rho_h = \sqrt[5]{\frac{\text{res}_h^l}{\text{res}_h^{l-5}}} \tag{7}$$

where l denotes the final iteration. The stopping criterion is chosen as the absolute residual over all unknowns to be less than 10^{-6}. Table I presents the reduction factors and the number of iterations required for multigrid $F(1,1)$-cycles, (meaning one pre- and one post-smoothing iteration). The smoothing method for each of the equations in the transformed system is the red–black Gauss–Seidel iteration. The table shows that the multigrid convergence with the distributive smoother is independent of the size of parameter λ and independent of mesh size h. These properties are highly desirable and the average reduction factors of 0.11 are highly satisfactory. A converged solution is obtained in a split second.

Remark
We would like to mention that a coupled Vanka smoother, centered at the cell centers, also shows a multigrid convergence independent of the size of parameters λ and h. The convergence factor for an $F(1,1)$-cycle is about 0.19 in this case. The cost of this iteration is, however, approximately a factor of 4 higher than with the distributive smoother.

3. LINEAR ELASTICITY, MIXED FORMULATION

In this section, we consider, as a next problem with a dominating grad–div operator, a linear elasticity problem for homogeneous and isotropic, almost incompressible, material:

$$\begin{aligned} \mu\,\mathbf{rot}\,\text{rot}\,\mathbf{u}-(\lambda+2\mu)\,\mathbf{grad}\,\text{div}\,\mathbf{u}=\mathbf{f}, &\quad \mathbf{x}\in\Omega \\ \mathbf{u}(\mathbf{x})=\mathbf{g}, &\quad \mathbf{x}\in\Gamma \end{aligned} \tag{8}$$

where λ and μ, the Lamé coefficients, are related to Young's modulus E and Poisson's ratio ν by

$$\lambda=\frac{\nu E}{(1+\nu)(1-2\nu)}, \quad \mu=\frac{E}{2(1+\nu)}$$

It is well known that, in the incompressible limit where Poisson's ratio ν tends to 0.5 (or λ tends to infinity), the discretization needs to be stabilized and that the convergence rate of multigrid methods

DOI: 10.1002/nla

with standard smoothers deteriorates. In the incompressible limit, we deal with a dominating grad–div operator. The construction of robust multigrid methods for this problem has been considered by several authors. Schöberl [20] combined a specialized blockwise smoother with stable intergrid transfer operators to get a robust multigrid for nearly incompressible elasticity by the P2/P0 finite element discretization. Wieners [21] transferred a saddle point smoother for the Stokes problem [22] to the elasticity system and obtained a robust multigrid method for nearly incompressible elasticity problems.

We depart from a stable discretization, which is given by a mixed formulation, see, for example, Brezzi–Fortin [23], introducing a new variable $p=-\lambda(\operatorname{div}\mathbf{u})$ in (8):

$$\begin{aligned} \mu\,\mathbf{rot}\operatorname{rot}\mathbf{u}-2\mu\,\mathbf{grad}\operatorname{div}\mathbf{u}+\mathbf{grad}\,p&=\mathbf{f}, \quad \mathbf{x}\in\Omega\\ \operatorname{div}\mathbf{u}+\lambda^{-1}p&=0, \quad \mathbf{x}\in\Omega\\ \mathbf{u}(\mathbf{x})&=\mathbf{g}, \quad \mathbf{x}\in\Gamma \end{aligned} \tag{9}$$

The corresponding discrete problem reads as

$$\begin{aligned} \mu\,\mathbf{rot}_h\operatorname{rot}_h\mathbf{u}_h-2\mu\,\mathbf{grad}_h\operatorname{div}_h\mathbf{u}_h+\mathbf{grad}_h\,p_h&=\mathbf{f}_h\\ \operatorname{div}_h\mathbf{u}_h+\lambda^{-1}p_h&=0 \end{aligned} \tag{10}$$

The distributive smoothing procedure we propose here for discrete system (10) is defined in the following way: First, we introduce the *help variables* $\mathbf{w}_h=(\overline{\mathbf{w}}_h,q_h)$ as

$$\begin{pmatrix}\mathbf{u}_h\\ p_h\end{pmatrix}=\mathbf{C}_h\begin{pmatrix}\overline{\mathbf{w}}_h\\ q_h\end{pmatrix}=\begin{pmatrix}I & -\mathbf{grad}_h\\ \mu\operatorname{div}_h & -2\mu\operatorname{div}_h\mathbf{grad}_h\end{pmatrix}\begin{pmatrix}\overline{\mathbf{w}}_h\\ q_h\end{pmatrix}$$

The transformed system, $\mathbf{L}_h\mathbf{C}_h\mathbf{w}_h=\mathbf{f}_h$, then reads

$$\begin{pmatrix}\mu(\mathbf{rot}_h\operatorname{rot}_h-\mathbf{grad}_h\operatorname{div}_h) & 0\\ \left(1+\dfrac{\mu}{\lambda}\right)\operatorname{div}_h & -\left(1+\dfrac{2\mu}{\lambda}\right)\operatorname{div}_h\mathbf{grad}_h\end{pmatrix}\begin{pmatrix}\overline{\mathbf{w}}_h\\ q_h\end{pmatrix}=\begin{pmatrix}\mathbf{f}_h\\ 0\end{pmatrix}$$

Hence, we deal with a *triangular system* during smoothing and have Laplace-type operators on its diagonal. Basic pointwise Gauss–Seidel smoothing procedures for the operators on the main diagonal are the methods of choice, where we start with the $(1,1)$-block and use these results in block $\mathbf{LC}_{h,2,1}$ before processing the $(2,2)$-block. Its excellent smoothing properties can be confirmed, for example, by LFA techniques.

We consider an elasticity problem with a simple analytic solution given by

$$u(x,y)=\cos(\pi x)\sin(\pi y)$$

$$v(x,y)=\sin(\pi x)\cos(\pi y)$$

Source term $\mathbf{f}$ and boundary conditions are consequently determined. The stopping criterion is chosen as the absolute residual over all unknowns to be less than 10^{-5}. The smoothing method for each of the equations in the transformed system is again the red–black Gauss–Seidel iteration. Table II presents the $F(1,1)$ multigrid convergence factors, ρ_h, and the number of multigrid

DOI: 10.1002/nla

Table II. $F(1,1)$ multigrid convergence factors, ρ_h, and in brackets the number of iterations, for different v-values in the elasticity test problem.

Grid	32×32	64×64	128×128	256×256
$v=0.25$	0.13 (14)	0.13 (14)	0.13 (14)	0.13 (14)
$v=0.4$	0.13 (14)	0.13 (14)	0.13 (14)	0.13 (14)
$v=0.45$	0.13 (15)	0.13 (14)	0.13 (14)	0.13 (14)
$v=0.49$	0.13 (15)	0.13 (15)	0.13 (15)	0.13 (15)
$v=0.499$	0.13 (16)	0.13 (16)	0.13 (16)	0.13 (16)

iterations required with the proposed smoother for Young's modulus $E=3\times 10^4$ and different values of v. A fast and robust multigrid convergence in the limit $v\to 0.5$ can be observed. We also mention that the $V(1,1)$-cycle also performs very well with convergence factors of 0.18 for $v=0.499$ for different mesh sizes.

4. SECONDARY CONSOLIDATION BIOT'S MODEL

Classical soil consolidation theory addresses the time-dependent coupling between the deformation of a porous matrix and the fluid flow inside. The porous matrix is supposed to be saturated by the fluid phase and the flow is governed by Darcy's law. The state of the continuous medium is characterized by the knowledge of the displacements and the fluid pressure at each point of the domain. One assumes the material's solid structure to be linearly elastic, initially homogeneous, and isotropic; the strains imposed within the material are small. Correspondingly, the displacements are assumed to be small. The consolidation process under 1D conditions was first investigated by Terzagui [24] and a phenomenological model was proposed and analyzed by Biot [25] in 3D.

For a rather general consolidation process, an elastic response of the soil skeleton to the loads is assumed. A change in stress will generate a deformation and an excess of the pore pressure. The dissipation of pressure will then result in a final deformed state of the porous matrix. This is, however, not really realistic for situations in which the soil deformation continues even though all excess pore pressure has been dissipated. This phenomenon is typical in the consolidation of clay soils. The presence of this process, *the secondary consolidation*, can be explained by assuming that the soil skeleton is governed by a viscoelastic behavior. We, therefore, consider Biot's secondary consolidation model. A mathematical model has been formulated by Murad and Cushman [26] and reported in [27]. If we denote by $\mathbf{u}$ the displacement vector and by p the pore pressure of the fluid, the governing equations for a homogeneous, isotropic, and incompressible medium, describing secondary consolidation, read

$$\begin{aligned} -\lambda^*\mathbf{grad}(\operatorname{div}\mathbf{u})_t-\operatorname{div}\boldsymbol{\sigma}+\alpha\mathbf{grad}\,p&=\mathbf{g}(\mathbf{x},t)\\ \alpha(\operatorname{div}\mathbf{u})_t-\kappa\Delta p&=f(\mathbf{x},t)\\ \boldsymbol{\sigma}(\mathbf{u})=\lambda(\operatorname{div}\mathbf{u})I+2\mu\boldsymbol{\varepsilon}(\mathbf{u}),\quad \mathbf{x}\in\Omega,\ \ 0<t&\leqslant T \end{aligned} \tag{11}$$

where $(\cdot)_t$ denotes the time derivative, λ^* is the secondary consolidation parameter, λ and μ are the Lamé coefficients, κ is the hydraulic conductivity, α is the Biot–Willis coefficient, I denotes

DOI: 10.1002/nla

the identity operator, and $\boldsymbol{\varepsilon}(\mathbf{u})$ is the strain tensor

$$\varepsilon_{i,j}(\mathbf{u}) = \frac{1}{2}\left(\frac{\partial u_i}{\partial x_j} + \frac{\partial u_j}{\partial x_i}\right) \tag{12}$$

In the sequel, we will assume that $\alpha = 1$, $f(\mathbf{x}, t) \in L^2(\Omega)$ and $\mathbf{g}(\mathbf{x}, t) \in (L^2(\Omega))^2$.

To complete the formulation of a well-posed problem, we must add appropriate boundary and initial conditions. For this purpose, let us take two partitions of the boundary Γ in complementary parts $\{\Gamma_d, \Gamma_f\}$ and $\{\Gamma_c, \Gamma_t\}$. We will suppose that the clamped boundary Γ_c has a non-null measure. Common boundary conditions for a solution of problem (11) are

$$\begin{aligned} p &= 0 \quad \text{on } \Gamma_d \\ k(\nabla p)\cdot\mathbf{n} &= 0 \quad \text{on } \Gamma_f \\ \mathbf{u} &= \mathbf{0} \quad \text{on } \Gamma_c \\ \lambda^*(\operatorname{div}\mathbf{u})_t\mathbf{n} + \boldsymbol{\sigma}\mathbf{n} - \alpha p\mathbf{n} &= \mathbf{t} \quad \text{on } \Gamma_t \end{aligned} \tag{13}$$

where $\mathbf{n}$ is the unit outward normal to the boundary Γ. At initial time, $t = 0$, the following initial condition is given

$$(\operatorname{div}\mathbf{u})(\mathbf{x}, 0) = 0, \ \ \mathbf{x} \in \Omega \tag{14}$$

Existence and uniqueness of the solution of problem (11)–(14) have been analyzed by Showalter [28] and Barucq *et al.* [29].

After semi-discretization in time using a two-weighted level scheme, we encounter, also here, a problem with a dominant grad–div operator at each time level, if the time step is sufficiently small.

4.1. Discrete formulation

The numerical solution of the Biot problems is usually obtained by using finite element methods; see, for instance, the monograph by Lewis and Schrefler [30]. Problems where the solution is smooth are satisfactorily solved by standard discretizations. Nevertheless, when strong pressure gradients occur, these methods are unstable in the sense that strong non-physical oscillations appear in the approximation of the pressure field. It is well known that this phenomenon appears at the beginning of the consolidation process when a load is applied on a part of the boundary. After this initial phase, the solution shows a much smoother behavior. The oscillatory behavior of the FEM can be reduced if stabilized methods are used. As for the Stokes problem, approximation spaces for the vector and the scalar fields, satisfying the LBB stability condition [31], can be used. This approach has been analyzed in [32–34] by Murad *et al.* and Mira *et al.* [35] for the quasi-static Biot's model. However, these methods still present pressure oscillations, when very sharp boundary layers occur; see [8], where the Taylor–Hood method on the 1D Terzaghi problem has been evaluated. In [36] a combination of the least-square mixed finite element method and local grid refinement near the load boundary was used to obtain non-oscillatory solutions.

Standard finite difference schemes, as finite elements, suffer from the same unstable behavior in their pressure approximation. A reason for this instability has been identified in [8, 9], where

DOI: 10.1002/nla

the use of a *staggered grid discretization* for poroelasticity problems was proposed, leading to oscillation-free solutions for any value of the discretization parameters. Stabilization techniques, based on either a problem reformulation or on the addition of artificial terms to the original equations, can be found in [19, 37], respectively.

The approach for the numerical approximation of the secondary consolidation problem (11) here is based on staggered finite differences. Often, if the problem of interest permits, staggered finite difference methods lead to discretizations that mimic the continuous problem, so that the main properties of the continuous problem are preserved in the discrete case. The consolidation problems of interest are typically defined on large block-shaped domains, ideally suited for Cartesian grids and finite differences. This discretization on Cartesian grids can also be combined with local refinement in order to capture the pressure boundary layer more accurately. We do not employ local refinement here, but the multigrid components proposed can naturally be incorporated in the multilevel adaptive technique [38] or the full adaptive composite method [39].

The secondary consolidation problem (11) can be expressed in a coordinate-free form using the operators divergence, gradient, and rotation in the following way:

$$\begin{aligned} -\lambda^* \mathbf{grad}(\operatorname{div}\mathbf{u})_t + \mu\,\mathbf{rot}\operatorname{rot}\mathbf{u} - (\lambda+2\mu)\,\mathbf{grad}\operatorname{div}\mathbf{u} + \mathbf{grad}\,p = \mathbf{g} \\ (\operatorname{div}\mathbf{u})_t - \kappa \operatorname{div}\mathbf{grad}\,p = f(\mathbf{x},t), \quad \mathbf{x}\in\Omega, \;\; 0<t\leqslant T \end{aligned} \tag{15}$$

where the operators rot and **rot** were defined in the 2D case in Section 2.1. For simplicity in our presentation, we consider Dirichlet boundary conditions for displacements and pressure. We assume a unique sufficiently regular solution in $(0,T]\times\Omega$ to exist.

In poroelasticity problems, pressure values are often prescribed at the physical boundary. Hence, pressure points in the staggered grid should be located at the physical boundary, and the displacement points are then defined at the cell faces. The staggered discretization in space has been described in various publications [9, 40], including a proof of convergence.

For (15), we also consider a staggered grid in time. Let M be a positive integer, $\tau = T/M$ the time step, and $\{t_m = m\tau\}_{m=0}^{M}$, $\{t_{m+1/2} = (m+1/2)\tau\}_{m=0}^{M-1}$ the time levels where the displacements and the pressure are approximated, respectively (see Figure 3). On this staggered mesh in time, using a second-order two-weighted level scheme, we define the following discrete problem:

$$-\lambda^*\,\mathbf{grad}_h \operatorname{div}_h \frac{\mathbf{u}_h^{m+1}-\mathbf{u}_h^m}{\tau} + (\mu\,\mathbf{rot}_h \operatorname{rot}_h - (\lambda+2\mu)\,\mathbf{grad}_h \operatorname{div}_h)\left(\frac{\mathbf{u}_h^{m+1}+\mathbf{u}_h^m}{2}\right)$$

$$+\mathbf{grad}_h\, p_h^{m+1/2} = \left(\frac{\mathbf{g}_h^{m+1}+\mathbf{g}_h^m}{2}\right)$$

$$\operatorname{div}_h \frac{\mathbf{u}_h^{m+1}-\mathbf{u}_h^m}{\tau} - \operatorname{div}_h \mathbf{grad}_h\, p_h^{m+1/2} = f_h^{m+1/2}, \quad m=0,\ldots M-1$$

$$\operatorname{div}_h \mathbf{u}_h^0(0) = 0$$

where the discrete operators have been introduced in Section 2.

DOI: 10.1002/nla

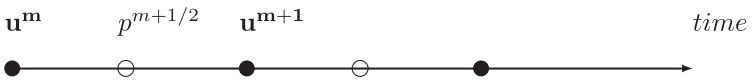

Figure 3. Staggered mesh in time. Grid points for displacement • at time t_m and for pressure ∘ at time $t_{m+1/2}$.

4.2. *Distributive smoothing, secondary consolidation*

For the secondary consolidation problem, at each time step we have to solve the discrete problem:

$$\tau\mu\,\mathbf{rot}_h\,\mathrm{rot}_h\,\mathbf{u}_h-(2\lambda^\star+\tau(\lambda+2\mu))\,\mathbf{grad}_h\,\mathrm{div}_h\,\mathbf{u}_h+2\tau\,\mathbf{grad}\,p_h=\widetilde{\mathbf{g}}_h \tag{16}$$

$$\mathrm{div}_h\,\mathbf{u}_h-\tau\kappa\,\mathrm{div}_h\,\mathbf{grad}_h\,p_h=\widetilde{f}_h \tag{17}$$

For the distributive smoothing of system (16)–(17), we define new help variables by

$$\begin{pmatrix}\mathbf{u}_h\\ p_h\end{pmatrix}=\begin{pmatrix} I & -\mathbf{grad}_h\\ \left(\dfrac{\lambda^*}{\tau}+\dfrac{\lambda+\mu}{2}\right)\mathrm{div}_h & -\left(\dfrac{\lambda^*}{\tau}+\dfrac{\lambda+2\mu}{2}\right)\mathrm{div}_h\,\mathbf{grad}_h\end{pmatrix}\begin{pmatrix}\overline{\mathbf{w}}_h\\ q_h\end{pmatrix}$$

The transformed system, $\mathbf{L}_h\mathbf{C}_h$, for secondary consolidation then reads

$$\mathbf{L}_h\mathbf{C}_h=\begin{pmatrix}\tau\mu(\mathbf{rot}_h\,\mathrm{rot}_h-\mathbf{grad}_h\,\mathrm{div}_h) & 0\\ \mathrm{div}_h-\kappa\left(\lambda^*+\dfrac{(\lambda+\mu)\tau}{2}\right)\Delta_h\,\mathrm{div}_h & -\Delta_h+\kappa\left(\lambda^*+\dfrac{(\lambda+2\mu)}{2}\tau\right)\Delta_h^2\end{pmatrix}$$

This transformed operator is again triangular; hence, it is suited for decoupled smoothing. The operators occurring on the main diagonal are of Laplace and biharmonic type. By means of another help variable, we are able to split the biharmonic operator up, solely for smoothing and deal only with scalar Laplace-like operators (see, for example, [17]). Scalar red–black Gauss–Seidel iteration can be the smoother of choice here.

4.2.1. Coupled smoothing method. Coupled cellwise smoothing of unknowns in a staggered grid arrangement for poroelasticity is performed by updating the five unknowns (pressure $p_{i,j}$, 2 times u_h- and v_h-displacements, $u_{i+1/2,j}, u_{i-1/2,j}, v_{i,j+1/2}, v_{i,j-1/2}$), centered around a pressure point simultaneously. A small 5×5-matrix must be inverted for each cell. 'Cellwise' smoothing is shown in Figure 4(a). Note that the word 'cell' does not relate to a grid cell here, as the unknowns are centered around a pressure point. In one smoothing iteration, all displacement unknowns are updated twice, whereas pressure unknowns are updated once.

DOI: 10.1002/nla

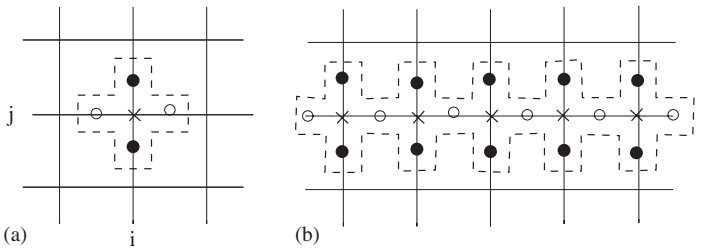

Figure 4. Five unknowns coupled smoothing: (a): cellwise and (b): x-linewise; $\times$, p_h; $\circ$, u_h; $\bullet$, v_h.

Figure 4(b) presents the linewise version of this smoother. The linewise versions can be performed in various orderings. The block matrices to be inverted are somewhat involved.

4.3. Numerical secondary consolidation experiment

We consider a 2D problem (15) defined on the unit square with Dirichlet boundary conditions. The source terms $\mathbf{g}(\mathbf{x}, t)$ and $f(\mathbf{x}, t)$ and the boundary and initial conditions are such that an analytic solution results:

$$u(x, y, t) = \cos(\pi x)\sin(\pi y)\sin(\pi t)$$

$$v(x, y, t) = \sin(\pi x)\cos(\pi y)\sin(\pi t)$$

$$p(x, y, t) = -2(\lambda+2\mu)\pi\sin(\pi x)\sin(\pi y)\sin(\pi t) - 2\pi^2\lambda^*\sin(\pi x)\sin(\pi y)\cos(\pi t)$$

To approximate this solution, we use a staggered grid in time and in space as described in Section 4.1. Second-order convergence in maximum norm for displacements and pressure is obtained for this problem with smooth analytical solution. In the numerical experiments, the parameter settings chosen are $\lambda=\mu=\lambda^*=k=1$ at final time $T=0.5$.

At each time level, the corresponding linear system is solved by multigrid. The measure of convergence is related to the absolute value of the residual after the mth iteration in the maximum norm over the three equations in the system:

$$\text{res}_h^m = |r_{1,h}^m| + |r_{2,h}^m| + |r_{3,h}^m|$$

where $r_{i,h}^m$ is the residual associated with the ith equation of the system. The multigrid convergence factor, ρ_h, is again given by (7). The stopping criterion is chosen as the absolute residual over all unknowns to be less than 10^{-6}. A matrix-free, stencil-based version of multigrid is used.

In Table III we display the $V(1,1)$- and $F(1,1)$-multigrid convergence factors, ρ_h, for several smoothers employing different time steps ($\tau=10^{-1}, 10^{-2}, 10^{-3}$). We only present the multigrid convergence of the first time step as it is representative for the other time steps as well. We compare the coupled Gauss–Seidel and Vanka smoothers, in their cellwise (**GS_point**, **V_point**) and the line-cell (**GS_line**, **V_line**) versions, with the pointwise and linewise versions of the distributive

DOI: 10.1002/nla

Table III. $V(1,1)$- and $F(1,1)$-multigrid convergence factors, ρ_h, for the secondary consolidation problem.

		Smoother					
Cycle	τ	**GS_point**	**GS_line**	**V_point**	**V_line**	**D_point**	**D_line**
$V(1,1)$	10^{-1}	0.783	0.259	0.658	0.216	0.389	0.113
	10^{-2}	0.901	0.766	0.836	0.720	0.397	0.113
	10^{-3}	0.902	>1	0.810	0.786	0.403	0.114
$F(1,1)$	10^{-1}	0.734	0.212	0.575	0.182	0.230	0.010
	10^{-2}	0.877	0.739	0.844	0.690	0.231	0.011
	10^{-3}	0.926	0.843	0.918	0.785	0.233	0.007

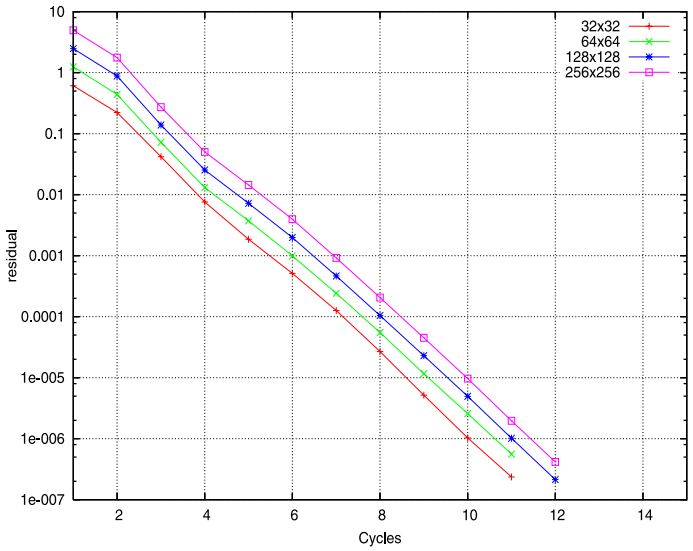

Figure 5. Multigrid convergence $F(1,1)$-cycle, $\tau = 10^{-3}$, pointwise-distributive.

smoothing methods (**D_point**, **D_line**). From Table III, we observe that the **GS_point** and **V_point** smoothers are not appropriate for this kind of problem and that the **GS_line** and **V_line** smoothers have a satisfactory behavior for large values of τ. However, their performance degrades when the time step becomes sufficiently small. The distributive smoothers, on the contrary, show a robust behavior independent of the size of the time step. Moreover, the **D_line** smoother gives significantly better convergence factors than the **D_point** smoother.

We now focus on the **D_point** and **D_line** smoothers with $\tau = 10^{-3}$ and varying the meshsize in space. The $F(1,1)$-cycle is applied at each time step. The multigrid convergence during the first time step for different numbers of spatial mesh points $32 \times 32, \ldots, 256 \times 256$ is presented in Figures 5 and 6, respectively, for **D_point** and **D_line**. In both figures, we observe that, independent of the

DOI: 10.1002/nla

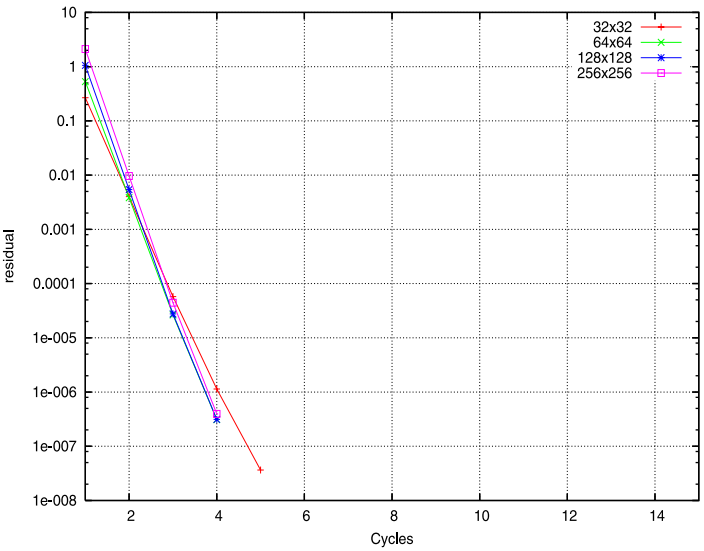

Figure 6. Multigrid convergence $F(1,1)$-cycle, $\tau = 10^{-3}$, linewise-distributive.

mesh size, the residual in norm is very small after very few iterations showing the robustness and efficiency of these smoothers. The central processing unit time for this problem on a Pentium IV, 2.6 MHz, is 1.5 s per time step on a 128^2-grid and 6 s per time step on a 256-grid. As in [17], we also expect here to obtain similar multigrid convergence factors for a wide range of poroelasticity parameters.

5. 3D LINEAR POROELASTICITY PROBLEM

The final grad–div dominating problem treated in this paper is a 3D linear poroelasticity problem for a nearly incompressible material. The mathematical formulation of this model is a particular case of the system considered in (16) corresponding to parameter $\lambda^* = 0$. Hence, the classical Biot's primary consolidation problem can be expressed in coordinate-free form as

$$\mu\,\mathbf{rot}\,\mathbf{rot}\,\mathbf{u} - (\lambda + 2\mu)\,\mathbf{grad}\,\mathrm{div}\,\mathbf{u} + \mathbf{grad}\,p = \mathbf{g}(\mathbf{x}, t)$$

$$(\mathrm{div}\,\mathbf{u})_t - \kappa\,\mathrm{div}\,\mathbf{grad}\,p = f(\mathbf{x}, t), \quad \mathbf{x} \in \Omega, \quad 0 < t \leqslant T \tag{18}$$

where the operator **rot** is defined in the usual way in 3D. With $\lambda \gg \mu$ we deal with grad–div dominating problems.

Here, we briefly outline the staggered grid in 3D, as we will show that the generalization of the multigrid solution method for linear poroelasticity to 3D is straightforward.

DOI: 10.1002/nla

The 3D staggered grid is composed of the following types of grid points:

$$\begin{aligned}
\overline{\omega}_n &= \{(ih, jh, kh),\ i,j,k=0,\ldots,N\}\\
\overline{\omega}_u &= \{((i+\tfrac{1}{2})h, jh, kh),\ i=-\tfrac{1}{2},0,1,\ldots,N-1,N-\tfrac{1}{2},\ j,k=0,\ldots,N\}\\
\overline{\omega}_v &= \{(ih,(j+\tfrac{1}{2})h, kh),\ i,k=0,\ldots,N,\ j=-\tfrac{1}{2},0,1,\ldots,N-1,N-\tfrac{1}{2}\}\\
\overline{\omega}_w &= \{(ih, jh,(k+\tfrac{1}{2})h),\ i,j=0,\ldots,N,\ k=-\tfrac{1}{2},0,1,\ldots,N-1,N-\tfrac{1}{2}\}\\
\overline{\omega}'_u &= \{(ih,(j+\tfrac{1}{2})h,(k+\tfrac{1}{2})h),\ i=0,\ldots,N,\ j,k=-\tfrac{1}{2},0,1,\ldots,N-1,N-\tfrac{1}{2}\}\\
\overline{\omega}'_v &= \{((i+\tfrac{1}{2})h, jh,(k+\tfrac{1}{2})h),\ j=0,\ldots,N,\ i,k=-\tfrac{1}{2},0,1,\ldots,N-1,N-\tfrac{1}{2}\}\\
\overline{\omega}'_w &= \{((i+\tfrac{1}{2})h,(j+\tfrac{1}{2})h, kh),\ k=0,\ldots,N,\ i,j=-\tfrac{1}{2},0,1,\ldots,N-1,N-\tfrac{1}{2}\}
\end{aligned} \tag{19}$$

The discrete operators used are

$$\mathrm{div}_h : H_{\overline{\omega}_u} \times H_{\overline{\omega}_v} \times H_{\overline{\omega}_w} \to H_{\overline{\omega}_n} \tag{20}$$

$$\mathbf{grad}_h : H_{\overline{\omega}_n} \to H_{\overline{\omega}_u} \times H_{\overline{\omega}_v} \times H_{\overline{\omega}_w} \tag{21}$$

$$\mathbf{rot}_h : H_{\overline{\omega}_u} \times H_{\overline{\omega}_v} \times H_{\overline{\omega}_w} \to H_{\overline{\omega}'_u} \times H_{\overline{\omega}'_v} \times H_{\overline{\omega}'_w} \tag{22}$$

$$\overline{\mathbf{rot}}_h : H_{\overline{\omega}'_u} \times H_{\overline{\omega}'_v} \times H_{\overline{\omega}'_w} \to H_{\overline{\omega}_u} \times H_{\overline{\omega}_v} \times H_{\overline{\omega}_w} \tag{23}$$

The divergence operator is naturally approximated by a central discretization of the displacements in a cell and the other discrete operators are defined in a standard way in the framework of staggered grids so that the compatibility relations $\mathbf{rot}_h\,\mathbf{grad}_h = 0$, $\mathrm{div}_h\,\overline{\mathbf{rot}}_h = 0$, are satisfied.

If we use a uniform grid for the discretization in time with step size $\tau > 0$ and employ an implicit Euler scheme, at each time step the following problem has to be solved:

$$\mu\,\overline{\mathbf{rot}}_h\,\mathbf{rot}_h\,\mathbf{u}_h^{m+1} - (\lambda+2\mu)\,\mathbf{grad}_h\,\mathrm{div}_h\,\mathbf{u}_h^{m+1} + \mathbf{grad}_h\,p_h^{m+1} = \widetilde{\mathbf{g}}_h \tag{24}$$

$$\mathrm{div}_h\,\mathbf{u}_h^{m+1} - \tau\kappa\,\mathrm{div}_h\,\mathbf{grad}_h\,p_h^{m+1} = \widetilde{f}_h \tag{25}$$

5.1. Distributive smoothing, linear poroelasticity

We consider distributive smoothing methods for the 3D linear poroelasticity problem with dominating grad–div operator. The distributive smoother for the discrete system of linear poroelasticity has been defined and evaluated in detail in 2D in [12, 17]. Here, we show that, as the multigrid convergence with this smoother is independent of problem parameters, it also works well in the case of dominating grad–div operators. We perform 3D computations here.

For distributive smoothing of system (24) and (25), we define the discrete help variables to be

$$\begin{pmatrix} \mathbf{u}_h \\ p_h \end{pmatrix} = \begin{pmatrix} I & -\mathbf{grad}_h \\ (\lambda+\mu)\,\mathrm{div}_h & -(\lambda+2\mu)\,\mathrm{div}_h\,\mathbf{grad}_h \end{pmatrix} \begin{pmatrix} \overline{\mathbf{w}}_h \\ q_h \end{pmatrix}$$

DOI: 10.1002/nla

The transformed system, $\mathbf{L}_h\mathbf{C}_h$, for primary consolidation then reads

$$\mathbf{L}_h\mathbf{C}_h = \begin{pmatrix} \mu(\overline{\mathbf{rot}}_h\,\mathbf{rot}_h - \mathbf{grad}_h\,\mathrm{div}_h) & 0 \\ \mathrm{div}_h - \kappa(\lambda+\mu)\tau\Delta_h\,\mathrm{div}_h & -\Delta_h + \kappa(\lambda+2\mu)\tau\Delta_h^2 \end{pmatrix}$$

Working in Cartesian coordinates in the 3D case, the distributor reads

$$\mathbf{C}_h = \begin{pmatrix} I_h & 0 & 0 & -(\partial_x)_{h/2} \\ 0 & I_h & 0 & -(\partial_y)_{h/2} \\ 0 & 0 & I_h & -(\partial_z)_{h/2} \\ (\lambda+\mu)(\partial_x)_{h/2} & (\lambda+\mu)(\partial_y)_{h/2} & (\lambda+\mu)(\partial_x)_{h/2} & -(\lambda+2\mu)\Delta_h \end{pmatrix} \tag{26}$$

with identity I_h. Hence, the transformed system reads

$$\mathbf{L}_h\mathbf{C}_h = \begin{pmatrix} -\mu\Delta_h & 0 & 0 & 0 \\ 0 & -\mu\Delta_h & 0 & 0 \\ 0 & 0 & -\mu\Delta_h & 0 \\ LC_h^{4,1} & LC_h^{4,2} & LC_h^{4,3} & \kappa(\lambda+2\mu)\tau\Delta_h^2 - \Delta_h \end{pmatrix} \tag{27}$$

with

$$LC_h^{4,1} = (\partial_x)_{h/2} - \kappa(\lambda+\mu)\tau((\partial_{xxx})_{h/2} + (\partial_{xyy})_{h/2} + (\partial_{xzz})_{h/2})$$

$$LC_h^{4,2} = (\partial_y)_{h/2} - \kappa(\lambda+\mu)\tau((\partial_{xxy})_{h/2} + (\partial_{yyy})_{h/2} + (\partial_{yzz})_{h/2})$$

and

$$LC_h^{4,3} = (\partial_z)_{h/2} - \kappa(\lambda+\mu)\tau((\partial_{xxz})_{h/2} + (\partial_{yyz})_{h/2} + (\partial_{zzz})_{h/2})$$

where the central discrete operators read in stencil notation

$$(\partial_x)_{h/2} \mathrel{\hat{=}} \frac{1}{h}[-1 \;\star\; 1]_h, \quad (\partial_{xxx})_{h/2} \mathrel{\hat{=}} \frac{1}{h^3}[-1 \;\; 3 \;\star\; -3 \;\; 1]_h$$

$$(\partial_{xxy})_{h/2} \mathrel{\hat{=}} \frac{1}{h^3}\begin{bmatrix} 1 & -2 & 1 \\ & \star & \\ -1 & 2 & -1 \end{bmatrix}_h$$

with $\star$ denoting the position on the grid at which the stencil is applied. The other discrete operators are given by analogous stencils.

The discrete linear poroelasticity system may contain anisotropies depending on the choice of the Lamé coefficients. The smoothing properties for the system are, however, not affected by these scalar anisotropies.

5.2. Numerical 3D linear poroelasticity experiments

Here, two 3D numerical experiments are considered.

DOI: 10.1002/nla

5.2.1. Squeezing a sponge. The first numerical problem corresponds to the simulation of a rubber sponge saturated with water with edges of length $2L$. The origin is placed at the center of the sponge and the coordinate axes are parallel to its edges. A load applied to it will produce a compression and the water will be squeezed out of the pores. This problem can be considered as a 3D generalization of the 1D Terzaghi problem [24]. The analytic solution of this problem is given by (see [41])

$$u(\mathbf{x},t)=\frac{u_0}{L}x+L\sum_{k=1}^{\infty}\gamma_k\sin\left(\frac{k\pi x}{L}\right)\exp\left(-\frac{k^2\pi^2 t}{C}\right)$$

$$p(\mathbf{x},t)=(\lambda+2\mu)\sum_{k=1}^{\infty}\gamma_k k\pi\exp\left(-\frac{k^2\pi^2 t}{C}\right)\left(\cos\left(\frac{k\pi x}{L}\right)+\cos\left(\frac{k\pi y}{L}\right)+\cos\left(\frac{k\pi z}{L}\right)\right)$$

where u_0 is a given constant value, $C=L^2(\kappa(\lambda+2\mu))^{-1}$, and $\gamma_k=(-1)^k 2u_0(Lk\pi)^{-1}$. The components v and w are calculated by replacing x for y and z, respectively. In Table IV, we display the convergence factors, ρ_h, and the number of iterations for different grids and values of ν, with ν tending to 0.5. We observe the robustness with respect to the parameters and good convergence for ν close to 0.5 (the grad–div dominating problem).

5.2.2. 3D footing problem. The last problem is a true 3D footing problem. The simulation domain is a $64\times64\times64$ m block of porous soil, $\Omega=(-32,32)\times(-32,32)\times(0,64)$, as in Figure 7.

Table IV. $F(2,1)$ multigrid convergence factors, ρ_h, and in brackets, the number of iterations, for different ν-values in the poroelasticity problem: squeezing a sponge.

Grid	$16\times16\times16$	$32\times32\times32$	$48\times48\times48$	$64\times64\times64$
$\nu=0.25$	0.07 (11)	0.07 (11)	0.07 (11)	0.07 (12)
$\nu=0.4$	0.07 (11)	0.07 (11)	0.07 (12)	0.07 (12)
$\nu=0.45$	0.07 (11)	0.07 (12)	0.07 (12)	0.07 (12)
$\nu=0.49$	0.07 (12)	0.07 (12)	0.07 (13)	0.07 (13)
$\nu=0.499$	0.07 (13)	0.07 (13)	0.07 (14)	0.07 (14)

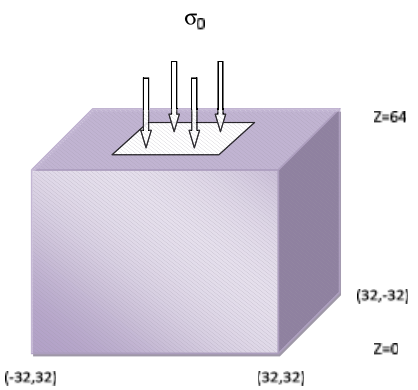

Figure 7. Domain of the 3D footing problem.

DOI: 10.1002/nla

Table V. Material parameters for the 3D poroelastic problem.

Property	Value	Unit
Young's modulus	3×10^4	N/m^2
Poisson's ratio	0.45	—
Permeability	10^{-7}	m^2
Fluid viscosity	10^{-3}	Pa s

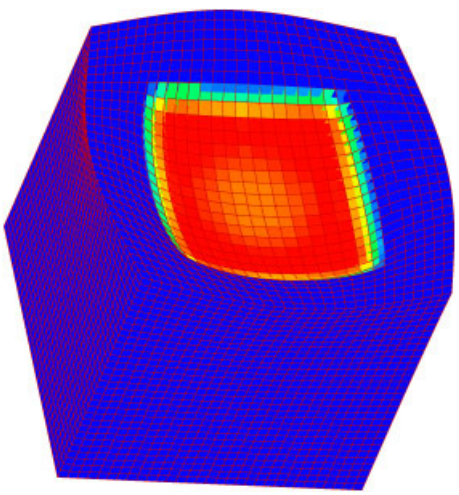

Figure 8. Numerical solution for pressure with the corresponding deformation at time $=0.5$ with a 32^3-mesh.

At the base of this domain, the soil is assumed to be fixed while at some centered upper part of the domain a uniform load of intensity $\sigma_0 = 0.1\,N/m^2$ is applied in a square of area $32 \times 32\,m^2$. The whole domain is assumed free to drain. The material properties of the porous medium are given in Table V.

In Figure 8, we show the numerical solution for the pressure and the corresponding deformation obtained with a 32^3-mesh at final time $T = 0.5$. The $F(2,1)$-cycle is applied at each time step with a line distributive smoother. The multigrid convergence for different numbers of spatial mesh points 16^3, 32^3, 48^3, and 64^3 is presented in Figure 9. We again confirm the robustness and efficiency of this smoother.

6. CONCLUSION

For systems of equations with a dominating grad–div term, the convergence factor of basic multigrid methods increases very quickly as the mesh size approaches zero. The reason is that some of the oscillatory eigenvectors lie at the low end of the spectrum. Basic smoothing methods perform well on the oscillatory eigenvectors at the high end of the spectrum. When not all oscillatory

DOI: 10.1002/nla

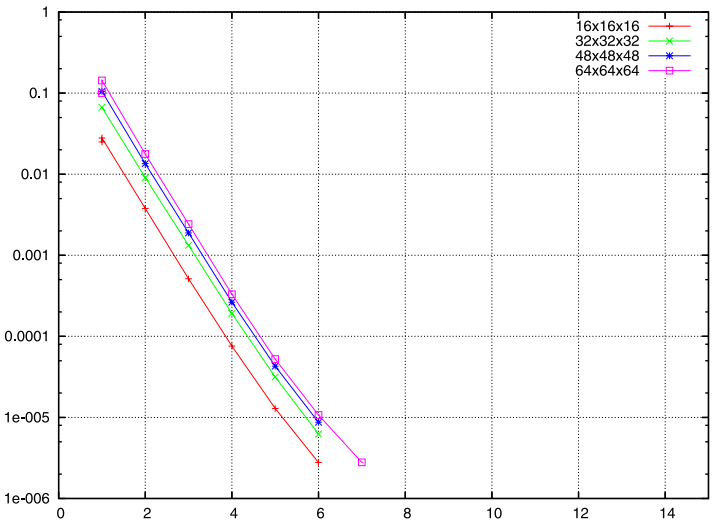

Figure 9. Multigrid convergence $F(2,1)$-cycle for the 3D footing problem, $\tau = 0.5$, linewise-distributive.

error components are reduced well enough, a coarse grid correction is useless, and multigrid does not converge well enough. By means of distributive smoothing methods, it is possible to design efficient smoothing procedures for some grad–div-dominated operators presented. After a transformation of the system, we can reduce all the high-frequency error components appearing in the systems of interest. The choice of discretization is an important one: On a staggered grid with finite differences the discrete divergence, curl, and gradient operators have similar properties as their continuous counterparts. This forms the basis for the success of distributive smoothing methods. Numerical experiments on model problems confirm this. For relatively complex systems of equations, we were able to produce textbook multigrid efficiency.

The distributive smoothers introduced in this paper heavily rely on transformations with discrete operators. It may, therefore, be nontrivial to generalize them to PDE problems with varying coefficients, as, for example, in [42]. However, since these smoothers can be implemented based only on local stencils, an idea for generalization is to apply the *transformations locally*. We have not yet tested this approach. Another generalization to be discussed is irregularly shaped domains. This should be possible with discretizations that preserve the important operator properties needed for distributive smoothing. Mimetic discretizations on triangular grids, for example, are candidates for efficient geometric multigrid methods based on this type of smoothing. This is part of forthcoming work.

REFERENCES

1. Olshanskii MA, Reusken A. Grad–div stabilization for Stokes equations. *Mathematics of Computation* 2004; **73**:1699–1718.
2. Arnold DN, Falk RS, Winther R. Multigrid in H(div) and H(curl). *Numerische Mathematik* 2000; **85**:197–217.
3. Vassilevski PS, Wang J. Multilevel iterative methods for mixed finite element discretizations for elliptic problems. *Numerische Mathematik* 1992; **63**:503–520.
4. Arnold DN, Falk RS, Winther R. Preconditioning in H(div) and applications. *Mathematics of Computation* 1997; **66**:957–984.

DOI: 10.1002/nla

5. Hiptmair R, Hoppe RHW. Multilevel methods for mixed finite elements in three dimensions. *Numerische Mathematik* 1999; **82**:253–279.
6. Hyman JM, Shashkov M. Adjoint operators for the natural discretizations of the divergence, gradient and curl on logically rectangular grids. *Applied Numerical Mathematics* 1997; **25**:413–442.
7. Hyman JM, Shashkov M, Steinberg S. The effect of inner products for discrete vector fields on the accuracy of mimetic finite difference methods. *Computers and Mathematics with Applications* 2001; **42**:1527–1547.
8. Gaspar FJ, Lisbona FJ, Vabishchevich PN. A finite difference analysis of Biot's consolidation model. *Applied Numerical Mathematics* 2003; **44**:487–506.
9. Gaspar FJ, Lisbona FJ, Vabishchevich PN. Staggered grid discretizations for the quasi-static Biot's consolidation problem. *Applied Numerical Mathematics* 2006; **56**:888–898.
10. Brandt A. Multigrid techniques: 1984 guide with applications to fluid dynamics. *GMD-Studie Nr. 85*, Sankt Augustin, Germany, 1984.
11. Trottenberg U, Oosterlee CW, Schüller A. *Multigrid*. Academic Press: London, 2000.
12. Wienands R, Gaspar FJ, Lisbona FJ, Oosterlee CW. An efficient multigrid solver based on distributive smoothing for poroelasticity equations. *Computing* 2004; **73**:99–119.
13. Lin P. A sequential regularization method for time-dependent incompressible Navier–Stokes equations. *SIAM Journal on Numerical Analysis* 1997; **34**:1051–1071.
14. Wittum G. Multi-grid methods for Stokes and Navier–Stokes equations with transforming smoothers: algorithms and numerical results. *Numerische Mathematik* 1999; **54**:543–563.
15. Wittum G. On the convergence of multi-grid methods with transforming smoothers. *Numerische Mathematik* 1990; **57**:15–38.
16. Brandt A, Dinar N. Multigrid solutions to flow problems. In *Numerical Methods for Partial Differential Equations*, Parter S (ed.). Academic Press: New York, 1979; 53–147.
17. Gaspar FJ, Lisbona FJ, Oosterlee CW, Wienands R. A systematic comparison of coupled and distributive smoothing in multigrid for the poroelasticity system. *Numerical Linear Algebra with Applications* 2004; **11**:93–113.
18. Vanka SP. Block-implicit multigrid solution of Navier–Stokes equations in primitive variables. *Journal of Computational Physics* 1996; **65**:138–158.
19. Gaspar FJ, Lisbona FJ, Oosterlee CW. A stabilized difference scheme for deformable porous media and its numerical resolution by multigrid methods. *Computing and Visualization in Science* 2008. DOI: 10.1007/s00791-007-0061-1.
20. Schöberl J. Multigrid methods for a parameter dependent problem in primal variables. *Numerische Mathematik* 1999; **84**:97–119.
21. Wieners C. Robust multigrid methods for nearly incompressible elasticity. *Computing* 2001; **64**:289–306.
22. Braess D, Sarazin R. An efficient smoother for the Stokes problem. *Applied Numerical Mathematics* 1997; **23**:3–19.
23. Brezzi F, Fortin M. *Mixed and Hybrid Finite Element Methods.* Springer: Berlin, 1991.
24. Terzaghi K. *Theoretical Soil Mechanics.* Wiley: New York, 1943.
25. Biot M. General theory of three dimensional consolidation. *Journal of Applied Physics* 1941; **12**:155–169.
26. Murad MA, Cushman JH. Multiscale flow and deformation in hydrophilic swelling porous media. *International Journal of Engineering Science* 1996; **3**:313–338.
27. Showalter RE. Diffusion in deforming porous media. *Dynamics of Continuous Discrete and Impulsive Systems—Series A*: *Mathematical Analysis* 2003; **10**:661–678.
28. Showalter RE. Diffusion in poroelastic media. *Journal of Mathematical Analysis and Applications* 2000; **251**: 310–340.
29. Barucq H, Madaune-Tort M, Saint-Macary P. On nonlinear Biot's consolidation models. *Nonlinear Analysis* 2005; **63**:985–995.
30. Lewis RW, Schrefler BA. *The Finite Element Method in the Static and Dynamic Deformation and Consolidation of Porous Media.* Wiley: New York, 1998.
31. Brezzi F. On the existence, uniqueness and approximation of saddle-point problems arising from Lagrange multipliers. *RAIRO—Modelisation Mathematique et Analyse Numerique* 1974; **8**:129–151.
32. Murad MA, Loula AFD. Improved accuracy in finite element analysis of Biot's consolidation problem. *Computer Methods in Applied Mechanics and Engineering* 1992; **95**:359–382.
33. Murad MA, Loula AFD. On stability and convergence of finite element approximations of Biot's consolidation problem. *International Journal for Numerical Methods in Engineering* 1994; **37**:645–667.
34. Murad MA, Thomée V, Loula AFD. Asymptotic behaviour of semi discrete finite-element approximations of Biot's consolidation problem. *SIAM Journal on Numerical Analysis* 1996; **33**:1065–1083.

35. Mira P, Pastor M, Li T, Liu X. A new stabilized enhanced strain element with equal order of interpolation for soil consolidation problems. *Computer Methods in Applied Mechanics and Engineering* 2003; **192**:4257–4277.
36. Korsawe J, Starke G, Wang W, Kolditz O. Finite element analysis of poro-elastic consolidation in porous media: standard and mixed approaches. *Computer Methods in Applied Mechanics and Engineering* 2006; **195**:1096–1115.
37. Gaspar FJ, Lisbona FJ, Oosterlee CW, Vabishchevich PN. An efficient multigrid solver for a reformulated version of the poroelasticity system. *Computer Methods in Applied Mechanics and Engineering* 2007; **196**:1447–1457.
38. Brandt A. Multi-level adaptive solutions to boundary-value problems. *Mathematics of Computation* 1977; **31**: 333–390.
39. McCormick SF. *Multilevel Adaptive Methods for Partial Differential Equations*. Frontiers in Applied Mathematics, vol. 6. SIAM: Philadelphia, 1989.
40. Gaspar FJ, Gracia JL, Lisbona FJ, Vabishchevich PN. A stabilized method for a secondary consolidation Biot's model. *Numerical Methods for Partial Differential Equations* 2008; **24**:60–78.
41. Kaasschieter EF, Frijns AJH. Squeezing a sponge: a three-dimensional analytic solution in poroelasticity. *Computational GeoSciences* 2003; **7**:49–59.
42. Ewing RE, Iliev OP, Lazarov RD, Naumovich A. On convergence of certain finite volume difference discretizations for 1D poroelasticity interface problems. *Numerical Methods for Partial Differential Equations* 2007; **23**:652–671.

DOI: 10.1002/nla